Structural relaxation in a molten salt probed by time-dependent dc conductivity measurements

Andrei Pimenov, Alois Loidl, R. Böhmer

Angaben zur Veröffentlichung / Publication details:

Pimenov, Andrei, Alois Loidl, and R. Böhmer. 1997. "Structural relaxation in a molten salt probed by time-dependent dc conductivity measurements." *Journal of Non-Crystalline Solids* 212 (1): 89–94. https://doi.org/10.1016/s0022-3093(97)00088-4.

Letter to the Editor

Structural relaxation in a molten salt probed by time-dependent dc conductivity measurements

A. Pimenov [a], A. Loidl [a], R. Böhmer [b,*]

[a] *Universität Augsburg, Experimentalphysik V, D86135 Augsburg, Germany*
[b] *Institut für Physikalische Chemie, Johannes Gutenberg-Universität, D55099 Mainz, Germany*

Abstract

Time-dependent dc conductivity was measured after cooling steps of about 2 K in the glass transformation range of $2Ca(NO_3)_2$–$3RbNO_3$. The shape and time scale of the *structural* relaxation function was thus monitored for times 60 s $< t <$ 10^6 s. The time scale could be compared with results from scanning calorimetry measurements and good agreement was found. From the heat capacity data and from the solid state conductivity the expected liquid state conductivity relaxation time was calculated using several models. The good compatibility of these calculations with the experimental results provides evidence that near the calorimetric glass transition the mobile ions perform concerted motions.

In many glass formers the structural rearrangements and the ionic mobility are fully coupled. If however the ion dynamics are strongly decoupled from the kinetics of the embedding random structure, the long range ionic motion in these *fast* ion conducting glasses can be of technological interest [1]. Particularly interesting from a more fundamental point of view are vitreous ionic materials for which the (isothermal) degree of decoupling can be modified by external parameters, such as the time variable. Here glass formers are required in which the ions are coupled to the amorphous structure, but only relatively loosely. For such substances two questions immediately arise which deal in quite different ways with the transition from the partially coupled, non-ergodic to the more fully coupled, ergodic state. First, how do initially decoupled ions recouple to the structural relaxation upon equilibration? And, second, is it possible to predict material properties in the more coupled liquid phase, from the behavior in the (decoupled) glassy state.

In order to address the first question the structural relaxation must be studied. This is often done through temperature [2] or pressure scanning investigations [3,4] usually employing the entropy variable, but other electrically or optically accessible quantities have been used as well; for some recent examples see, for example, Refs. [5,6]. Structural relaxations can also be induced by sudden temperature or pressure variations. Corresponding studies have been documented for refractory materials [7], amorphous polymers [8], other materials [9–11].

We have used a quasi-isothermal T-step method to monitor structural recoupling of the ionic motions

* Corresponding author. Tel.: +49-6131 392 536; fax: +49-6131 394 196; e-mail: bohmer@pc-aak.chemie.uni-mainz.de.

through dc conductivity investigations. Out of the small number of intermediately coupled ion conductors we have chosen $2Ca(NO_3)_2$–$3RbNO_3$ (CRN) [12]. This glass former which is similar to the often studied $2Ca(NO_3)_2$–$3KNO_3$ [13] is well suited because its conductivity response is much more strongly coupled [1] to the structural relaxation than in alkali-oxide melts. These materials have previously been studied using the conductivity monitored structural relaxation method [14–16]. As will be shown below the choice of the nitrate melts allows one to obtain low-noise conductivity monitored structural response functions with T steps as small as 2 K (rather than 30–50 K [14–16]). Furthermore the pronounced non-Arrhenius behavior of the relaxation times in the nitrate melts makes them valuable test cases in order to distinguish several models which allow prediction of liquid state properties based upon the vitreous state behavior.

Samples were prepared [12] and characterized by differential scanning calorimetry (DSC) using a Perkin Elmer DSC-4 at heating rates of 10 K/min after cooling from the molten state at rates between 1 and 100 K/min. Standard calibration procedures were applied in order to obtain glass transition temperatures to within ± 0.5 K.

The time dependent conductivity σ was measured employing the Schlumberger 1260 Gain-Phase analyzer equipped with an additional high-impedance preamplifier in order to increase the sensitivity of the instrument at low frequencies (The preamplifier incorporates a dedicated feedback network. The design of the preamplifier and the calibration procedure are similar to those described by Ref. [17].) The sample was placed between polished stainless steel plates (diameter 20 mm; electrode gap 2 mm). Due to uncertainties in the determination of the exact sample geometry the reported conductivities are only accurate to within $\pm 10\%$. During the experiments the capacitor assembly was maintained under N_2 atmosphere.

The measurement frequency was chosen to be 0.1 Hz. This value is convenient as is apparent from the analysis of reported conductivity spectra [7] represented for low frequencies in the upper insert of Fig. 1. One can see that for temperatures in the vicinity of

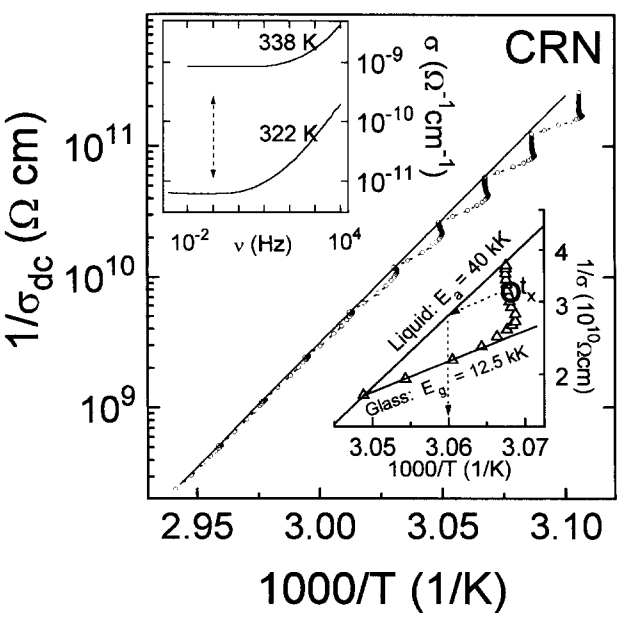

Fig. 1. Arrhenius plot of the dc conductivity represented as solid line [12]. The dots represent measurements from several runs each of which involves stepping the temperature by about 2 K downwards and then recording σ_{dc}. The upper insert depicts the conductivity dispersion in the relevant temperature range. The lower insert serves to illustrate how the fictive temperature is obtained from the data. The effective energy barriers in the annealed liquid, E_a, and in the glassy state, E_g, are represented by solid lines.

the glass transition the frequency of 0.1 Hz is located in the plateau regime of the conductivity. Thus measurements at a single frequency allow detection of dc conductivities σ which are affected neither by blocking electrode phenomena nor by conductivity dispersion.

Prior to the conductivity measurements the sample was heated to temperatures near 550 K and held for about 1 h. Runs which showed indications of crystallization during subsequent cooling (as evidenced by a precipitous drop in σ) were discarded. The explicitly time-dependent experiments were then carried out in the temperature range 340–320 K using the following procedure. The temperature was stabilized, but now at about $T_e + 2$ K with a relative accuracy of about 0.01 K. After an extended annealing period the temperature was rapidly lowered by about 2 K and the time dependent dc conductivity was recorded for times to 1×10^6 s. The characteristic time constant of the temperature controlling system was about 60 s.

In Fig. 1 we present the results of our time-dependent dc conductivity measurements together with their equilibrium conductivities. Far above the calorimetric glass transition temperature the relaxation is so fast, that the changes in conductivity directly follow those in temperature. This means that the time scale set by the experiment is longer than the structural relaxation time and the sample is always in metastable equilibrium. At lower temperatures, the structural relaxation becomes slower and one needs to increase the measurement time in order to achieve full equilibration at the new temperature. At still lower temperatures time of more than 10^6 s ($\sim$ 12 days) is not enough to allow the equilibrium to be reached. The lower insert of Fig. 1 illustrates how the fictive temperature $T_f(t)$ was obtained from $\sigma(t)$. To be more specific this was done as follows. As soon as the thermodynamic temperature was stabilized the instantaneous conductivity $\sigma(t_x)$, cf. Fig. 1, was converted into a fictive temperature by drawing a line with a slope E_g through the $\sigma(t_x)$ data point. The abscissa value where this line intersects that which represents the liquid state conductivity (marked by E_a in Fig. 1) corresponds to the fictive temperature $T_f(t_x)$. Immediately after a quench $\sigma(t)$ is evolving under 'constant structure' conditions and the temperature dependence of $\ln \sigma \propto E_g/T$ can be used to determine an activation energy $E_g \approx 12.5 \times 10^3$ K. This glassy state barrier is more than three times smaller than the effective barrier, E_a, determined for the annealed melt (cf. Fig. 1).

The explicit time dependence of the dc conductivity of CRN along with the temporal evolution of the measured sample temperature is shown for several T_e in Fig. 2. It is clearly seen that at the higher temperature (upper frame) the dc conductivity closely follows the changes in T. At the lower temperature two different decays in $\sigma(t)$ can be distinguished. One notes first a fast variation of the conductivity which directly follows the equilibration of the sample temperature and for later times a slow relaxation that reflects the internal approach of the sample towards structural equilibrium. This is because the ionic conductivity depends on the local activation energies set up by the environment of the mobile ions. This energy landscape obviously changes during equilibration; thus time dependence of the dc conductivity at T_e reveals information concerning *structural* relaxation. This means that by measuring $\sigma_{dc}(t)$ subsequent to a temperature jump one is able to determine

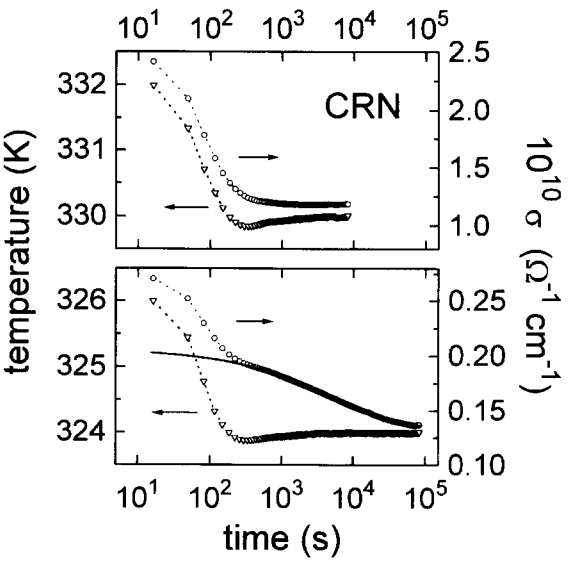

Fig. 2. Temporal evolution of sample temperature (left hand scale) and dc conductivity (right hand scale) shown for two different base temperatures. The solid line is a fit using the stretched exponential function to the data for equilibration times $t > 10^3$ s. The dashed lines represent the normalized variation of the thermodynamic sample temperature.

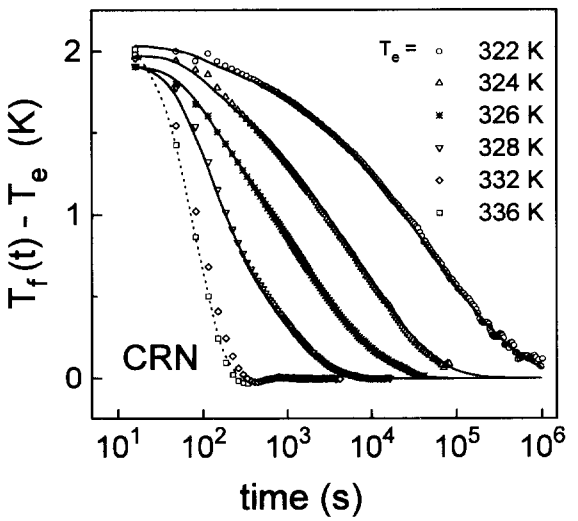

Fig. 3. Time dependence of the fictive temperature as obtained from dc conductivity data for several base temperatures T_e. The solid lines are calculated using Eqs. (1a) and (1b) and the parameters given in the text. The dashed line is a guide to the eye only.

the relaxation of fictive temperature $T_f(t)$. This is a somewhat unusual way of obtaining this quantity which is often measured by monitoring the temporal evolution of enthalpy, volume, index of refraction, etc.

Fig. 3 shows the relaxation of the fictive temperature in CRN as a function of time for different sample temperatures. At the lowest temperatures the time scales for thermalization and for structural equilibration are well separated. Here the fictive temperature relaxation could simply be described by a Kohlrausch law $T_f(t) - T_e = \Delta T \exp[-(t/\tau)^\beta]$ with a stretching exponent β and ΔT equaling $T_f(0) - T_e$. In the general case the non-ideality of the T step can be modeled via the coupled Narayanaswamy–Moynihan equations [2,9]

$$T_f(t) = T(t) - \int_{t_0}^{t} dt' \exp\left\{ -\left(\int_{t'}^{t} \frac{dt''}{\tau(t'')} \right)^\beta \right\}, \quad (1a)$$

$$\tau(t) = \tau_0 \exp\left(\frac{\Delta H x}{T(t)} + \frac{\Delta H (1-x)}{T_f(t)} \right). \quad (1b)$$

Here x is the so-called non-linearity parameter, τ_0 is a pre-exponential factor, and ΔH is an effective activation energy associated with structural relaxation [1]. It should be noted that there has been some controversy concerning the order of integrations and exponentiation in Eq. (1a). which yields distinguishable results only for T-step experiments employing an increase in temperature [2,18].

In order to obtain the solid lines in Fig. 3 we have solved Eqs. (1a) and (1b) numerically with τ_0, β and x as fit parameters. We find a stretching exponent $\beta \approx 0.51$ independent of temperature in the range investigated (within experimental error this exponent agrees well with those from the linear and non-linear enthalpy relaxation of the related glass-former CKN see Ref. [19] as well as Refs. [20,21]). The effective activation energy $\Delta H = 8.3 \times 10^4$ K as well as $\log_{10}(\tau_0/s) = -107$ were determined self-consistently from the temperature dependence of $\tau(T, t \to \infty)$. It turned out that for the parameters given the agreement between fits and data is only weakly sensitive to particular choices of the coefficient x in the range $0.3 \leq x \leq 0.5$. For the calculations shown in Fig. 3 we adopted $x = 0.31$, the average value found by Moynihan et al. [19] from DSC measurements of the structurally related glass former CKN. This insensitivity of the present experiment with regard to the non-linearity parameter is to be expected since only relatively small temperature steps were employed and thus the departure from the equilibrium state was not very large.

In order to compare the structural relaxation, measured using the conductivity method, with the enthalpy relaxation, we have performed DSC measurements on CRN. The insert of Fig. 4a shows a typical excess specific heat trace ΔC_p $(= C_{p,liquid} - C_{p,glass})$ and illustrates the method of equal areas [9] that we have used to the determine cooling-rate dependent glass transition temperatures $T_g(q)$. These yielded the enthalpy relaxation times via $\tau_S = kT_g^2/(q\Delta H)$ with $k \approx 30$ being an empirical constant [22]. Fig. 4a shows the similarity of the time constants obtained from both the enthalpy and the conductivity methods and therefore provides unambiguous evidence that

[1] It has be shown that instead of Eq. (1b) other functional forms involving at least three parameters can be used equally well, see Ref. [2]. But from the data shown in Fig. 4a the use of the two-parameter approach seems fully justified.

the latter can be used to sensitively monitor structural relaxation. The conductivity relaxation time $\tau_\sigma \propto \sigma^{-1}$ (for numerical details see Ref. [12]) corresponding to a cooling rate of about 0.5 K/min is also given. Fig. 4a documents the intermediate structure vs. ion mobility decoupling τ_σ/τ_s of $\sim 10^4$ at $T_g(10\ \mathrm{K/min}) = 332.5$ K.

In the following we will estimate the conductivity relaxation time in the liquid state from τ_σ in the solid. There are several models which allow such an estimate to be made [2]. One is based on the well known Adam–Gibbs equation which adapted for τ_σ reads for a linearly dependent excess specific heat $\Delta C_p = C_0 - C_1 T$ [23]

$$\tau_\sigma = \tau_0' \exp\{(Q/T)/[\ln(T_f/T_2) + C(T_f - T_0)]\}, \quad (2)$$

where $C \equiv C_1/C_0$ is taken from the experimental data (cf. Fig. 4a). The adjustable parameters are τ_0', Q, and T_2. It should be noted that in this expression T_f is T-dependent, with $T_f = T$ for $T > T_g(q)$ but fixed to T_g below this temperature. Alternatively Geyer et al. have suggested a scenario of concerted ionic motion in which the variation of the entropy associated with ΔC_p is thought to arise from liquid-like cells of those N ions which are responsible for the transport quantity under consideration [24]. Applying this model to the case of electrical conductivity one finds

$$\tau_\sigma = \tau_0'' \exp(E_s/T) \exp\left[N \int_0^T \Delta C_p/(RT)\, dt\right]. \quad (3)$$

Here E_s ($= E_g$, as given above) the effective barrier governing the T dependence of τ_σ in the solid state, and ΔC_p are both fixed experimentally. Again using the linear approximation for ΔC_p in the liquid state the second exponential term in Eq. (3) is given by $\exp\{N[C_0 \ln(T/T_g) + C_1(T - T_g)]\}$. Below T_g it is unity, since by definition ΔC_p vanishes for $T < T_g$. In Eq. (3) one has the parameters N, τ_0'', and E_s with the latter two being unambiguously fixed by the solid state conductivity data.

[2] Due to the pronounced curvature in τ_σ (cf. Fig. 5), an approach based on the Arrhenius law, like we have chosen above, clearly would be inadequate here.

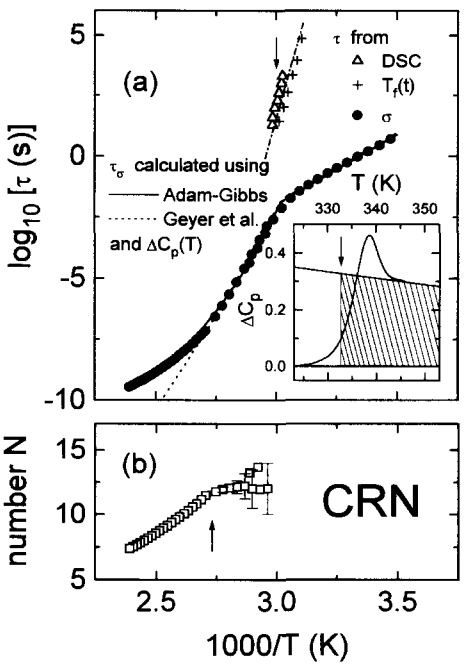

Fig. 4. (a) Conductivity relaxation times (●) and structural relaxation times (from $\sigma_{dc}(t)$ and from DSC). The slope dashed–dotted line gives the effective energy barrier, ΔH, associated with the structural relaxation. Solid and dotted lines reflect results from calculations using the Adam–Gibbs Eq. (2) and that given by Geyer et al., Eq. (3), respectively. The latter is not in accord with the experimental results for $T > 365$ K for constant N. The inset shows the excess specific heat of CRN measured for $q = 10$ K/min. The dashed area serves to illustrate the method of equal areas used to determine T_g (indicated by the arrows). Above $T = 350$ K, ΔC_p continues to decrease approximately linearly (not shown). (b) Cooperativity parameter N estimated from τ_σ using Eq. (3).

Using Eqs. (2) and (3) we have calculated the expected liquid state τ_σ and obtain, as shown in Fig. 4a, the solid and the dotted lines, respectively. The best fits are $Q = (1390 \pm 200)$ K and $T_2 = (255 \pm 10)$ K in the first case and $N = 12 \pm 1$ in the latter. Both times one finds 10^{-19} s for the pre-exponential factors with an estimated uncertainty of about two decades. Fig. 4a shows that the Adam–Gibbs based approach fits over the entire range over which heat capacity data were taken ($T < 410$ K). The other *ansatz* fails above $T \approx 365$ K, at least if N is kept constant. Of course a perfect match between experiment and model calculation can be achieved if N is allowed to vary, as shown in Fig. 4b. Note that

below T_g Eq. (3) is of course independent of N. It is quite remarkable that the temperature at which N starts to decrease significantly upon heating is identical to the critical temperature $T_C = 365$ K that was estimated from a mode-coupling analysis of the high-frequency conductivity data taken on $2Ca(NO_3)_2$–$3RbNO_3$ [25].

In conclusion we find that, after sufficiently long equilibration, initially decoupled, mobile ions in molten $2Ca(NO_3)_2$–$3RbNO_3$ fully recouple to the relatively slow rearrangements of the embedding amorphous structure. The response function $\Phi(t)$ associated with this process exhibits considerable stretching ($\beta = 0.51$). Only relatively small T steps were needed to obtain an excellent signal-to-noise-ratio. Using two different approaches, both based on the notion of concerted ionic motions, it was possible to achieve a unified description of the ion conduction in glass *and* liquid. The conclusion that this type of cooperative charge carrier motion, seen here in CRN, also governs ion freezing in other intermediately coupled amorphous electrolytes is yet to be substantiated by future investigations

Acknowledgements

We are indebted to A. Maiazza for assistance with sample preparation and to I. Alig and M. Vogt for making accessible the DSC equipment. C.A. Angell and K.L. Ngai are thanked for bringing Refs. [14–16] to our attention. This research was partly supported by the Sonderforschungsbereich 262.

References

[1] C.A. Angell, Ann. Rev. Phys. Chem. 43 (1992) 693.
[2] I.M. Hodge, J. Non-Cryst. Solids 169 (1994) 211, and references cited therein.
[3] P.K. Gupta, J. Non-Cryst Solids 102 (1988) 231.
[4] C. Alba-Simionesco, J. Chem. Phys. 100 (1994) 2250.
[5] H.-J. Winkelhahn, Th.K. Servay, D. Neher, Ber. Bunsenges. Phys. Chem. 100 (1996) 123.
[6] H. Wagner, R. Richert, Polymer 38 (1997) 255.
[7] H.N. Ritland, J. Am. Ceram. Soc. 39 (1956) 403.
[8] L.C.E. Struik, Physical Ageing in Amorphous Polymers and Other Materials (Elsevier, Amsterdam, 1978).
[9] C.T. Moynihan et al., Ann. N.Y. Acad. Sci. 279 (1976) 15.
[10] C.A. Angell, J. Non-Cryst. Solids 102 (1988) 205.
[11] H. Fujimori, H. Fujita, M. Oguni, Bull. Chem. Soc. Jpn. 68 (1995) 447.
[12] A. Pimenov, P. Lunkenheimer, M. Nicklas, R. Böhmer, A. Loidl, C.A. Angell, submitted to J. Non-Cryst. Solids.
[13] A. Pimenov, P. Lunkenheimer, H. Rall, R. Kohlhaas, A. Loidl, R. Böhmer, Phys. Rev. E54 (1996) 676, for a recent list of references.
[14] J. De Bast, P. Gilard, Phys. Chem. Glasses 4 (1963) 117.
[15] H. Kaneko, J.O. Isard, Phys. Chem. Glasses 9 (1968) 84.
[16] C.T. Moynihan et al., Fiz. Khim. Stekla 1 (1975) 420.
[17] R. Richert, Rev. Sci. Instrum. 67 (1996) 3217.
[18] R.W. Rendell, K.L. Ngai, G.R. Fong, J.J. Aklonis, Macromolecules 20 (1987) 1070.
[19] C.T. Moynihan, H. Sasabe, and J.C. Tucker, in: Proc. of the Int. Symp. on Molten Salts, ed. J.P. Pennsler, J. Bronstein, D.R. Morris, K. Nobe and W.P. Richards (Electrochemical Society, Pennington, NJ, 1976) p. 182.
[20] R. Böhmer, E. Sanchez, C.A. Angell, J. Phys. Chem. 96 (1992) 9089.
[21] Y.H. Jeong, I.K. Moon, Phys. Rev. B52 (1995) 6381.
[22] A. Pimenov, R. Böhmer, A. Loidl, Prog. Theor. Phys., in press.
[23] G.W. Scherer, J. Am. Ceram. Soc. 67 (1984) 504.
[24] U. Geyer et al., Phys. Rev. Lett. 75 (1995) 2364.
[25] P. Lunkenheimer, A. Pimenov, A. Loidl, to be published.